Materials Sciences and Applications, **2011, 2, 59-69**
doi:10.4236/msa.2011.22009 Published Online February 2011 (http://www.SciRP.org/journal/msa)

Development of Cockleshell-Derived $CaCO_3$ for Flame Retardancy of Recycled PET/Recycled PP Blend

Supaphorn Thumsorn[1], Kazushi Yamada[2], Yew Wei Leong[1], Hiroyuki Hamada[1]

[1]Department of Advanced Fibro-Science, Kyoto Institute of Technology, Kyoto, Japan; [2]Future Applied Conventional Technology Center, Kyoto Institute of Technology, Kyoto, Japan.
Email: nooh17@yahoo.com, kazushi@kit.ac.jp

Received December 24th, 2010; revised January 4th, 2011; accepted January 11th, 2011.

ABSTRACT

Recycled polyethylene terephthalate (*RPET*) *and recycle polypropylene* (*RPP*) *blends filled with a renewable filler*, *i.e. cockleshell-derived* $CaCO_3$ (*CS*) *were prepared as an environmental friendly thermoplastic composite. The effects of CS particle size and content on thermal stability*, *mechanical performance and flame retardant properties of the blends were investigated. Thermogravimetric analysis was performed to elucidate the thermal decomposition kinetics of the filled composites. The iso-conversion of the Flynn-Wall-Ozawa was developed by the second order polynomial function for thermal oxidative degradation of the blends while peak derivative temperature from the Kissinger method was able to verify the mechanism of degradation in these blends. The results indicated that both CS and commercial grade* $CaCO_3$ *improved thermal stability and enhanced the stiffness as well as impact performance of the blends. However*, *this could only be achieved when high filler content was present in the RPET/RPP blends.*

Keywords*: *Cockleshell*, *Aragonite* $CaCO_3$, *Thermal Decomposition Kinetic*, *Polymer Blend*, *Flame Retardancy

1. Introduction

According to environmental considerations, there is strong emphasis on using recycled and biodegradable polymers while using renewable fillers and additives to enhance their properties. Cockle, a type of bivalve mollusk, is one of the most popular seafood in Thailand. The large consumption of cockle has resulted in the cockleshells being left as garbage. The main mineral content in cockleshell is calcium carbonate ($CaCO_3$), which can be grinded into suitable particle sizes and incorporated as fillers in thermoplastics. The incorporation of cockleshell-derived $CaCO_3$ into thermoplastics is not only value adding to the shell but can also be a means of sustainable waste management strategy.

Polyethylene terephthalate (PET) and polypropylene (PP) have been widely used as drinking bottles and caps, respectively. Upon disposal, these materials are usually separated prior to recycling since they are regarded as immiscible. The compatibility of PET and PP blends, however, can be improved by using a suitable compatibilizer, such as styrene-ethylene-butadiene-styrene (SEBS) co-polymers, which yielded tougher and more thermally stable material [1-3]. However, the stiffness of the blends remained low, especially when there is high content of PP or compatibilizer. Therefore, one of the most promising methods to improve the mechanical performance of the blends is by the incorporation of fillers such as $CaCO_3$.

$CaCO_3$ mineral filler has been one of the most popular fillers used in the thermoplastic industry. $CaCO_3$ can be generally found in three distinct crystalline phases *i.e.* calcite, aragonite and vaterite. Calcite is the most stable and most commonly found in nature. Aragonite, however, can only be found in precipitate $CaCO_3$ or seashells whereas vaterite is found from synthesized $CaCO_3$ and does not occur naturally [4-6]. Generally, aragonite has higher density and hardness than calcite and vaterite, which makes it a valuable inorganic material that can be used as filler for armature plastic, rubber, paper, glass fiber, print ink, paint pigment and cosmetics [7].

Apart from mechanical properties, thermal stability is also one of the most important factors for processing of polymeric materials. Thermal decomposition kinetics of

Copyright © 2011 SciRes.

polymeric materials can be defined by kinetic parameters such as activation energy (E_a), pre-exponential factor (*ln* A) and reaction order (n). There are two basic thermal decomposition kinetic models including iso-conversion and peak derivative temperature for kinetic study, which is generally based on the Arrhenius equation [8-17]. The Flynn-Wall-Ozawa is a classical model of iso-conversion that can calculate E_a as a function of sample weight loss. On the other hand, the Kissinger model has been widely used for peak-derivative temperature calculation, which provides the kinetic parameters E_a, *ln* A and n for describing the thermal degradation stability.

In addition to thermal stability, the composites would also be evaluated based on their flammability, which is important should the material be considered for automotive and structural applications. The flame retardancy of CS filled RPET/RPP blend was investigated in order to further develop CS as an environmental friendly flame retardant material.

2. Experimental

2.1. Materials

The RPET and RPP in the form of flake from crushed waste bottles were provided by Yasuda Sangyo Co., Ltd, Japan. A finely ground commercial grade $CaCO_3$ (SOFTON1200) with an average particle size of 1.8 μm was purchased from Bihoku Funka Kogyo, Co., Ltd., Japan). Commercial grade $CaCO_3$ is hereby known as SOFTON. A styrene-ethylene-butadiene-styrene (SEBS) base compound was used as compatibilizer, which purchased from JSR Corporation, Japan.

Waste cockleshells were taken from Thailand and used as original without purification. The shells were washed, dried, ground and then sieved at 400 mesh size. Cockleshell derived-$CaCO_3$ is referred as "CS".

2.2. Sample Preparation

The ratios of RPET/RPP blends were set at 95/5, which was then compounded with 10 wt% CS and SOFTON in a single screw extruder (SRV-P70/62, Nihon Yuki Co., Ltd., Japan) with 5 phr (parts per hundred resin by weight) of SEBS based compatibilizer. RPET was dried by using a dehumidifying drier at 120˚C for 5 hours before compounding. The extruder barrel temperature was set at 260-285˚C at a screw speed of 50 rpm. The blends were dried by using an oven at 100˚C for 5 hours before being injection molded into dumbbell specimens by using a Po Yuen UM50 injection molding machine. The barrel temperature, injection speed and mold temperature during injection molding were set at 280˚C, 100 mm/s, and 30˚C, respectively.

2.3. Crystal Structure of $CaCO_3$ Fillers

Crystal structure of filler was determined by X-ray diffraction (XRD). The XRD intensity of the filler was collected from a JEOL/JDX 3530 diffractometer (Cu$K\alpha$) at a voltage of 30 kV and a filament current of 30 mA. The scans were made from 2θ = 5-60˚.

2.4. Morphology Observation

Morphology of fillers and blends was characterized by using a scanning electron microscope (JSM5200, JEOL, Japan). Gold coating was sputtered onto the specimens for electron conductivity.

2.5. Thermal Stability and Decomposition Kinetics

Thermogravimetric analysis (TGA) (TGA2950, TA Instruments) was performed to elucidate the thermal decomposition kinetics. The samples weighing between 3-5 mg was subjected to heating rates of 2, 5, 10 and 20˚C/min in nitrogen (N_2) and air. The kinetic parameters of thermal degradation of the blend was investigated by Flynn-Wall-Ozawa (FWO), Kissinger and Coats-Redfern methods, which the kinetic parameters are calculated from non-isothermal technique based on the Arrhenius equation and a solid stage reaction [8-17] by

$$\frac{d\alpha}{dT} = \frac{A}{\beta}\exp\left(\frac{E_a}{RT}\right) f(\alpha) \tag{1}$$

where A is the pre-exponential factor, β is a heating rate (˚C/min), E_a is activation energy (J/mol), R is a universal gas constant (8.314 J/mol K), T is absolute degradation temperature (K), $f(\alpha)$ is the reaction model and α is conversion of weight loss, which conversion from thermogravimetric study is expressed by

$$\alpha = \frac{m_0 - m_T}{m_0 - m_{final}} \tag{2}$$

where m_0 is initial mass, m_T is mass at decomposition temperature and m_{final} is mass at final decomposition reaction.

2.6. Limiting Oxygen Index

Flame retardant property of the blends was characterized by using limiting oxygen index (LOI) (ONI, oxygen index meter, Suga Test Instruments Co., Ltd., Japan) according to JIS K 7201-2, specimen type IV. The minimum concentration of oxygen in a flowing mixture of oxygen and nitrogen needed to continuously burn the sample for over 3 minutes or for a length of more than 50 mm was determined to be the LOI.

2.7. Mechanical Properties

Tensile test were performed by using an Instron 4206

Copyright © 2011 SciRes.

universal testing machine according to standard ASTM D638. The gauge length was 115 mm at an extension rate of 10 mm/min.

Izod impact strength was determined for 2 mm-deep notched specimens, which was cut from the parallel regions of the dumbbell specimens. The tests were conducted by using a Toyo Seiki Izod impact tester according to ASTM D256 with a pendulum of 5.50 J.

3. Results and Discussion

3.1. Characterization of Cockleshell-Derived $CaCO_3$

The average particle size of CS was measured from scanning electron microscopy (SEM) images. **Figure 1** shows SEM photographs and XRD patterns of $CaCO_3$ filler including CS and SOFTON. The average particle size of these fillers is presented in **Table 1**. It can be seen that the average particle size of CS after sieving was about 25 μm, which was larger than SOFTON.

The $CaCO_3$ content in CS was determined by heating the sample until 900˚C in a thermogravimetric analyzer at a heating rate of 20˚C/min under nitrogen atmosphere. A calculation of weight loss from $CaCO_3$ decomposition reveal that CS contains 97 wt% of $CaCO_3$, which is similar to that of SOFTON. Characterization of CS by X-ray diffraction revealed peaks at 2θ = 26.16˚ corresponding to (111) reflections from aragonite crystal structure of CS aragonite structures, as shown in **Figure 1(a)**. SOFTON, on the other hand, revealed peaks at 2θ = 29.44˚ corresponding to the (104) reflections of the calcite crystal structure as shown in **Figure 1(b)**.

3.2. Morphology of Filled RPET/RPP Blends

Figure 2 presents the SEM photographs of unfilled and filled RPET/RPP blend. All photographs exhibited good dispersion of RPP dispersed particles on RPET matrix, which attributed to compatibilization of the blend. The image J software was used to measure the sizes of the RPP dispersed phase in the blends. The average RPP dispersed particle sizes were 0.65, 0.48 and 1.60 μm for unfilled, SOFTON filled and CS filled RPET/RPP blends, respectively. The difference of RPP dispersed size should be considered due to the difference of interfacial tension between RPET/RPP and compatibilizer. The presence of filler in the blend increased the interfacial tension of RPET/RPP and compatibilizer due to interaction between filler and compatibilizer thus effect on coalescence of RPP dispersed phase particle. Therefore, CS filled RPET/RPP blend exhibited larger of RPP dispersed sizes as compared to others. However, smaller size of SOFTON would breakage RPP dispersed phase during compounding resulting in smaller RPP dispersed phase.

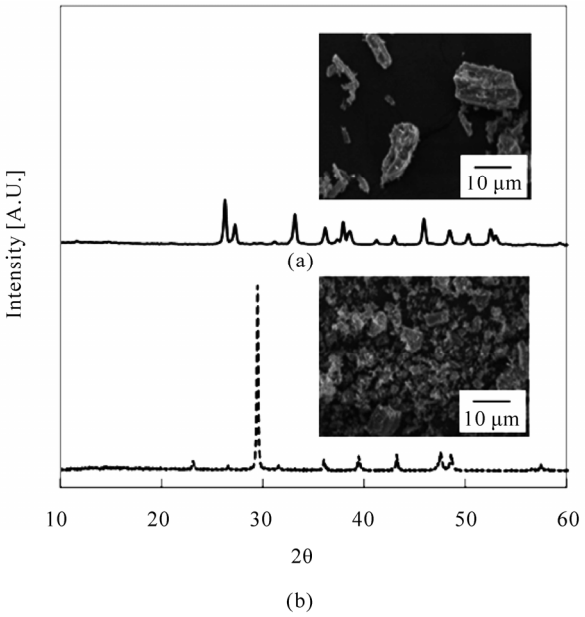

Figure 1. Structure and morphology of (a) CS and (b) SOFTON $CaCO_3$.

Table 1. Particle size and content of filler included thermal stability and E_a by Coats-Redfern equation.

Fillers	$CaCO_3$ content (%)	Average particle size (μm)	T_d onset (˚C)	T_d peak (˚C)	E_a (kJ/mol)
SOFTON	97.9	1.80	636.4	703.7	218.1
CS	97.5	25.2	608.1	697.1	180.6

3.3. Thermal Stability of Fillers

The effect of $CaCO_3$ filler particle size on its thermal stability and decomposition kinetic was determined through the Coats-Redfern equation by using a single heating rate at 20˚C/min in N_2. Thermal degradation temperature (T_d) and E_a values of the fillers are tabulated in **Table 1**. The results revealed that SOFTON exhibited better thermal stability than CS, as can be seen from the higher degradation temperature as well as E_a value. Low thermal stability of CS could be attributed to its lower heat transfer efficiency, which less capability for withstand high temperature, and corresponding to lower thermal stability of its aragonite than calcite $CaCO_3$ structure [4,6].

3.4. Thermal Decomposition Kinetic Study of RPET/RPP Blends

The typical effect of heating rate on non-isothermal degradation of the blends is presented in **Figure 3**. A shift in the conversion of weight loss (α) and peak derivative weight ($d\alpha/dt$) towards a higher temperature could be ob-

Copyright © 2011 SciRes.

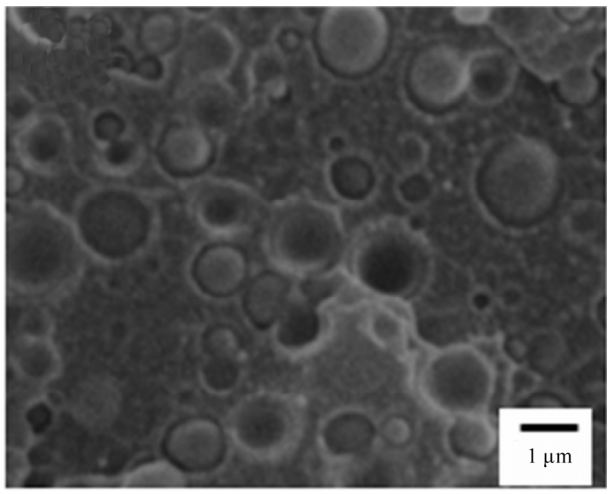

(a)

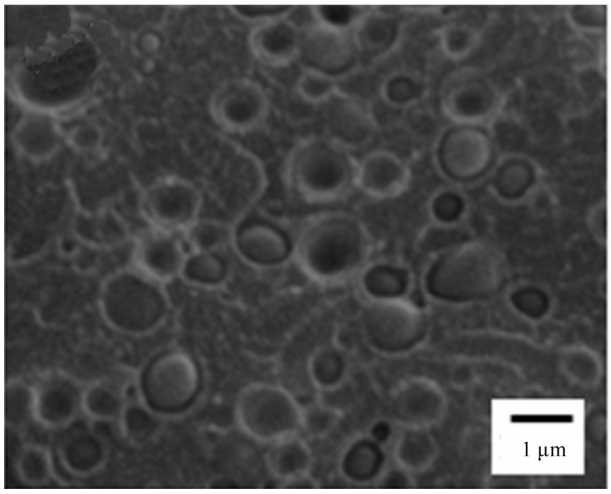

(b)

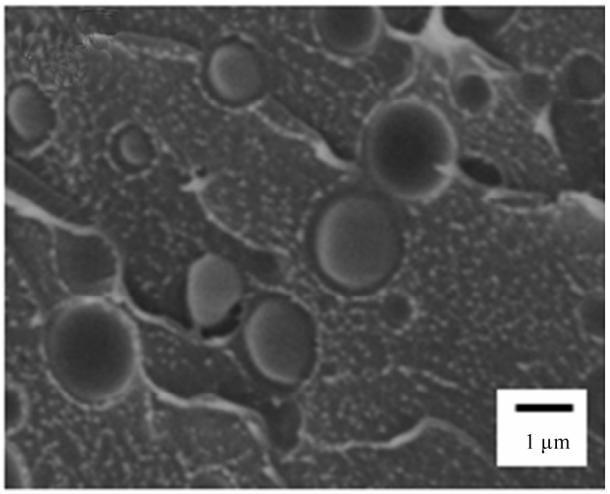

(c)

Figure 2. SEM photographs of (a) Unfilled (b) SOFTON filled and (c) CS filled RPET/RPP blends.

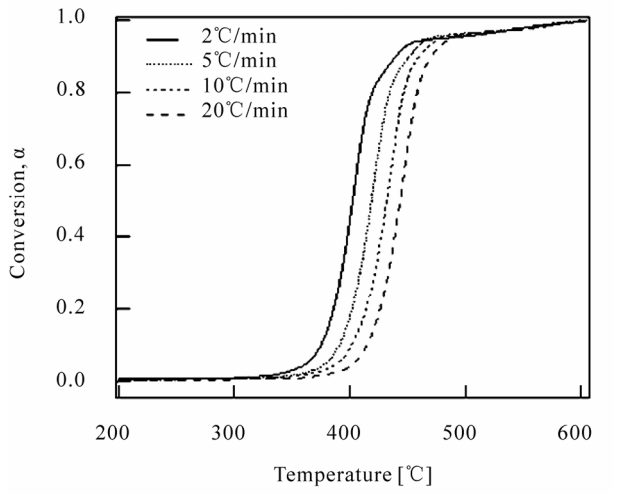

(a)

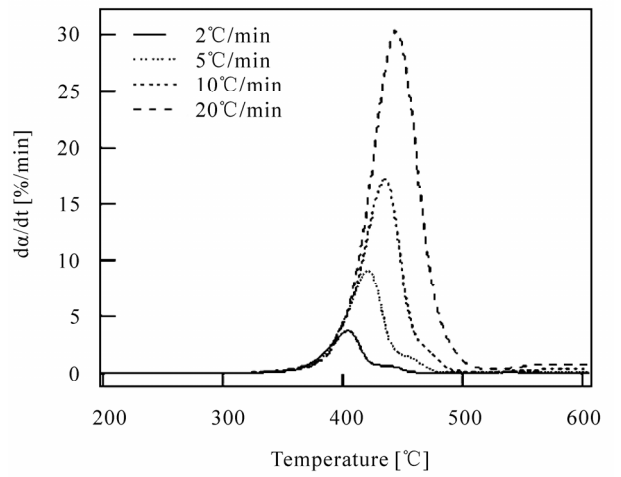

(b)

Figure 3. (a) Conversion and (b) Derivative weight TGA thermogram of CS filled RPET/RPP blend in N_2.

served when increasing heating rates. This was due to the lag in heat absorption by the specimens due to their relatively low thermal conductivity. However, the heating rates would significantly affect the thermal degradation of the samples. Therefore, it is necessary to use multi-heating rates when performing thermal decomposition kinetic studies.

Figures 4(a) and **(b)** compares the dα/dt curves of the samples degraded in N_2 and air, respectively. It was noted that the incorporation of both CS and SOFTON into RPET/RPP blends have resulted in a slight increase in the peak degradation temperature (T_d peak). Furthermore, it can be seen that degradation rate (dα/dt) of the blends decreased with the presence of both CS and SOFTON fillers. The increment of Td peak and reduction of dα/dt results indicated an improvement of thermal

Copyright © 2011 SciRes.

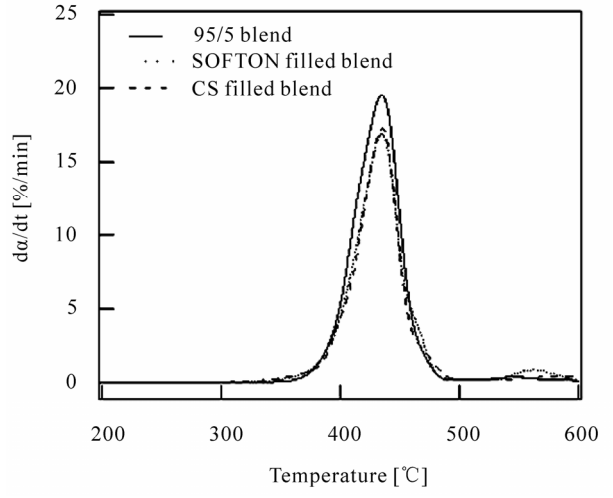

(a)

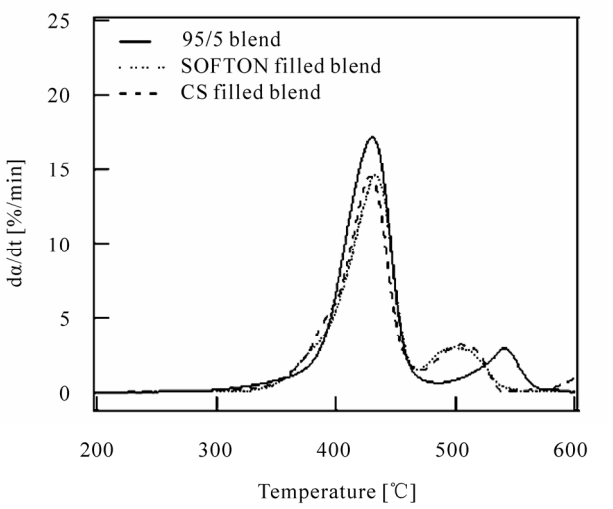

(b)

Figure 4. Derivative weight TGA thermograms of unfilled and filled RPET/RPP blends in (a) N_2 and (b) Air.

stability of the RPET/RPP. An obvious difference in thermal degradation mechanism could be observed, *i.e.* a single-step degradation in N_2 and two-step degradation in air. The decomposition mechanism of the blends can be explained by using thermal decomposition kinetics, which corresponds to solid state reaction models as tabulated in **Table 2**. The various kinds of models could be classified by isothermal plot between rate of reaction and conversion of the reaction. The shapes of the plot are corresponding to kinetic models and can be classified by acceleratory, decelerator, linear or sigmodal models, which are related to solid state kinetic models of nucleation, geometrical contraction, diffusion or reaction-order models as reviewed by Khawam *et al.* [11].

Figure 5 illustrates the isothermal plot of dα/dt and conversion of thermal decomposition (α) for the unfilled, CS- and SOFTON-filled RPET/RPP blends. The isothermal plot of dα/dt and α revealed a bell shaped curve whereby an initial increment of reaction rate was imminent with increasing conversion until a maximum decomposition reaction was reached, thereafter the reaction rate decreased until the decomposition process ended. The shape of these plots could be classified as sigmoidal models, which corresponds to reaction-order models [11]. Therefore, thermal decomposition kinetic of CS and SOFTON filled RPET/RPP blend can be evaluated based on the first-order reaction model by using Flynn-Wall-Ozawa and Kissinger model.

3.5. Thermal Decomposition Kinetic from Flynn-Wall-Ozawa

Thermal decomposition kinetic of Flynn-Wall-Ozawa (FWO) is an iso-conversion or model-free method, which can be calculated from the kinetic parameter by integral method through following equation

$$\log \beta = \log \frac{AE}{f(\alpha)R} - 2.315 - \frac{0.457E_a}{RT} \quad (3)$$

At constant heating rate, the kinetic parameter of activation energy can be calculated by using the slope of linear plots of log heating rate (β) and the inverse temperature ($1/T$) at various weight losses by

$$E_a = -\left(\frac{R}{0.457}\right)\left(\frac{d(\log \beta)}{d(1/T)}\right) \quad (4)$$

The thermal decomposition kinetic from Flynn-Wall-Ozawa yields linear plots between log β and $1/T$ based on Arrhenius relationship and their slopes are used for the calculation of kinetic parameters. **Figure 6** presents the linear relationship of unfilled, SOFTON filled and CS filled RPET/RPP blends during decomposition in N_2. The activation energy, E_a was directly evaluated from the slope of these plots.

Figure 7 shows the E_a values as a function of weight loss conversion of unfilled and filled RPET/RPP blends for thermal degradation in N_2. The E_a values at initial stage of decomposition (E_a 0.05) are 225, 218 and 191 kJ/mol while E_a values at 50% weight loss (E_a 0.50) are 237, 225 and 227 kJ/mol as tabulated in Table 3 for unfilled, SOFTON filled and CS filled REPT/RPP blends, respectively. The E_a values are almost constant from the initial stage until 50% weight loss, which indicates that a similar one-step thermal decomposition mechanism was true when the blends were degraded in N_2 thus confirming earlier decomposition profiles shown in **Figure 4(a)**. However, E_a values of CS filled RPET/RPP blend were

Copyright © 2011 SciRes.

Table 2. Solid state reaction and integral expressions for different reaction models.

Model	Differential form $f(\alpha) = 1/k\ d\alpha/dt$	Integral form $g(\alpha) = kt$
	Nucleation models	
Power law (P2)	$2\alpha^{1/2}$	$\alpha^{1/2}$
Power law (P3)	$3\alpha^{2/3}$	$\alpha^{1/3}$
Power law (P4)	$4\alpha^{3/4}$	$\alpha^{1/4}$
Avrami-Erofeyev (A2)	$2(1-\alpha)[-\ln(1-\alpha)]^{1/2}$	$[-\ln(1-\alpha)]^{1/2}$
Avrami-Erofeyev (A3)	$3(1-\alpha)[-\ln(1-\alpha)]^{2/3}$	$[-\ln(1-\alpha)]^{1/3}$
Avrami-Erofeyev (A4)	$4(1-\alpha)[-\ln(1-\alpha)]^{3/4}$	$[-\ln(1-\alpha)]^{1/4}$
Prout-Tompkins (B1)	$\alpha(1-\alpha)$	$\ln[\alpha/(1-\alpha)]+c^a$
	Geometrical contraction models	
Contracting area (R2)	$2(1-\alpha)^{1/2}$	$1-(1-\alpha)^{1/2}$
Ontracting volume (R3)	$3(1-\alpha)^{2/3}$	$1-(1-\alpha)^{1/3}$
	Diffusion Models	
1-D diffusion (D1)	$1/(2\alpha)$	α^2
2-D diffusion (D2)	$-[1/\ln(1-\alpha)]$	$((1-(1-\alpha)\ln(1-\alpha))+\alpha$
1-D diffusion-Jander (D3)	$[3(1-\alpha)^{2/3}]/[2(1-(1-\alpha)^{1/3})]$	$(1-(1-\alpha)^{1/3})^2$
Ginstling-Brounshtein (D4)	$3/[2((1-\alpha)^{/1/3}-1)]$	$(1-(2/3)\alpha-(1-\alpha)^{2/3}$
	Reaction order models	
Zero-order (F0/R1)	1	α
First-order (F1)	$(1-\alpha)$	$-\ln(1-\alpha)$
Second-order (F2)	$(1-\alpha)^2$	$[1/(1-\alpha)]$-1
Third-order (F3)	$(1-\alpha)^3$	$(1/2)[(1-\alpha)^{-2}-1]$

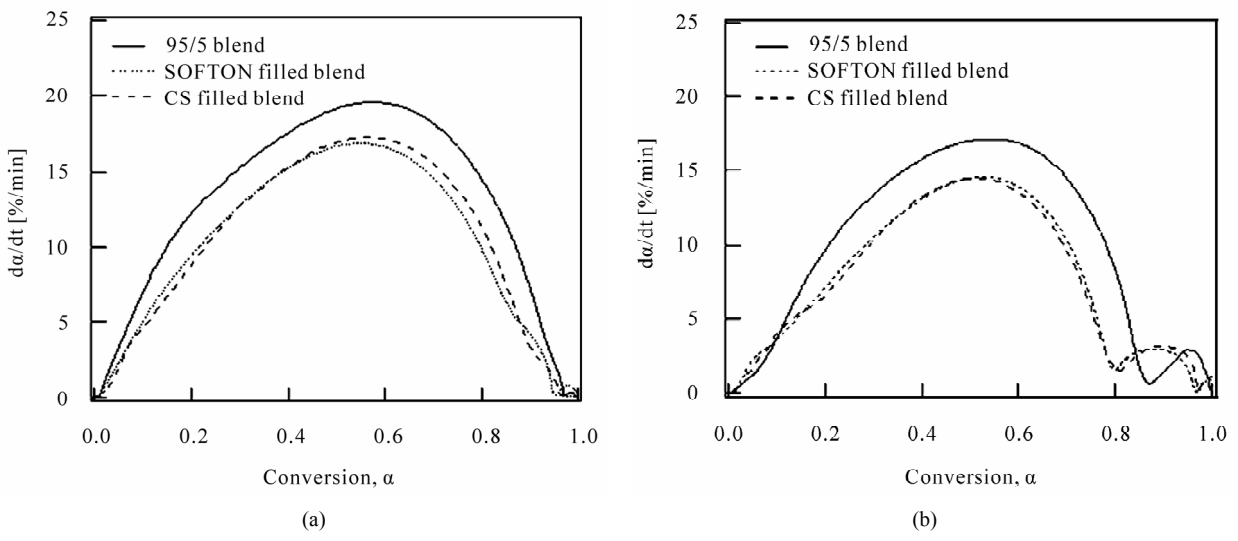

Figure 5. Isothermal plot of degradation rate and conversion decomposition of unfilled and filled RPET/RPP blends in (a) N_2 and (b) Air.

Copyright © 2011 SciRes.

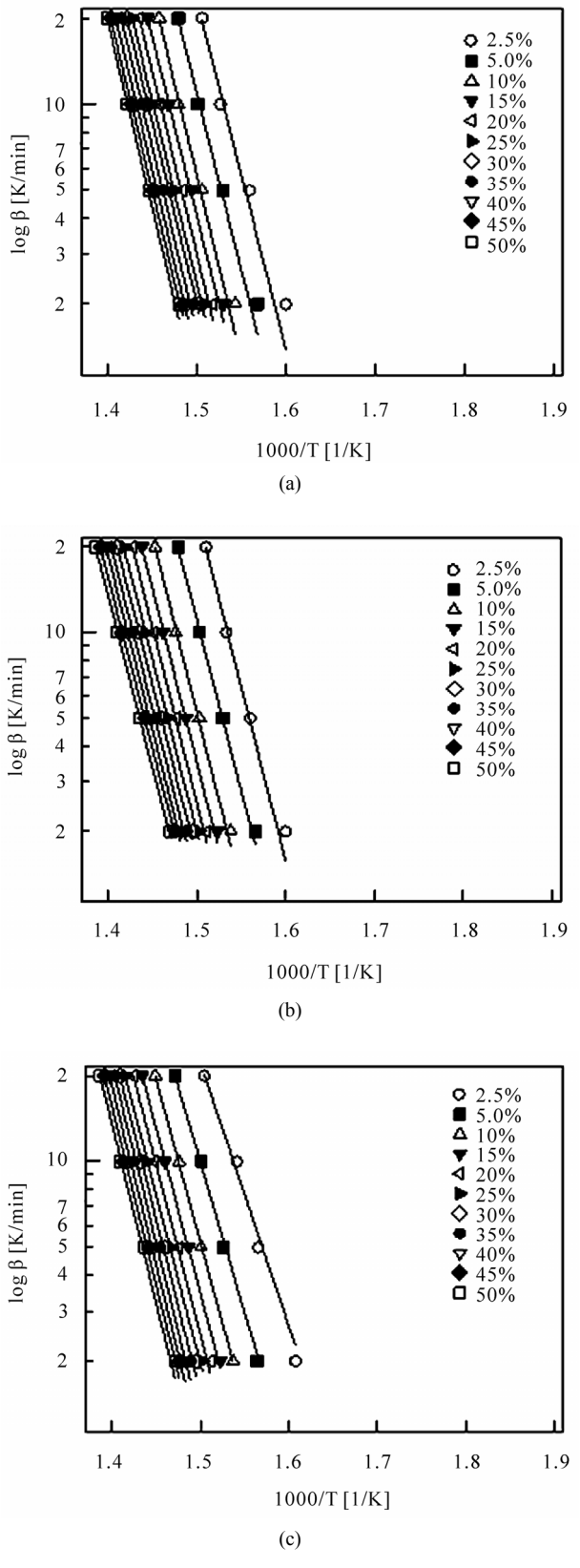

Figure 6. Flynn-Wall-Ozawa plot of (a) Unfilled (b) SOFTON filled and (c) CS filled RPET/RPP blends in N_2.

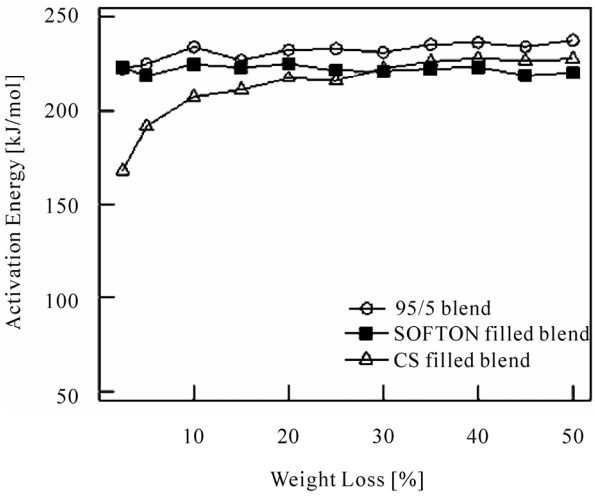

Figure 7. Activation energy of unfilled and filled RPET/ RPP blends in N_2.

lower than unfilled and SOFTON filled blends at the initial stage of decomposition, which suggest lower thermal stability of CS than SOFTON.

On the other hand, thermal oxidative degradation of these blends exhibited non-linear relationship between log β and $1/T$ of FWO plots for decomposition in the presence of O_2 as illustrated in **Figure 8**. Generally, the Flynn-Wall-Ozawa kinetic model enables the determination of E_a from the linear relationship of log β and $1/T$ from non-isothermal degradation at various heating rates. Nevertheless, thermal oxidative decomposition of unfilled and filled RPET/RPP blends from the FWO indicated some drawback of this method. Therefore, in this study the non-linear plot was successfully developed by using polynomial fitting data. These results are considered that E_a of thermal oxidative degradation was dependent on the slow heating rate and complex degradation mechanism [18]. The non linear relationship of these FWO plots can be fitted by using the second order polynomial function as described by

$$\log \beta = a\left[\frac{1}{T}\right]^2 + b\left[\frac{1}{T}\right] + c \qquad (5)$$

where a is polynomial coefficient, b is linear coefficient and c is constant.

The fitting plots revealed the curve of FWO plot at low heating rates, which was clearly seen at low weight loss decomposition. These results could be considered on the effect of particle size of filler as well as RPP dispersed phase particles on these blends, which attributed to their different surface areas. It can note that the decomposition reaction is significantly influenced by low heating rate, which this low heating rate decomposition can be explained and controlled the mechanism of the

Copyright © 2011 SciRes.

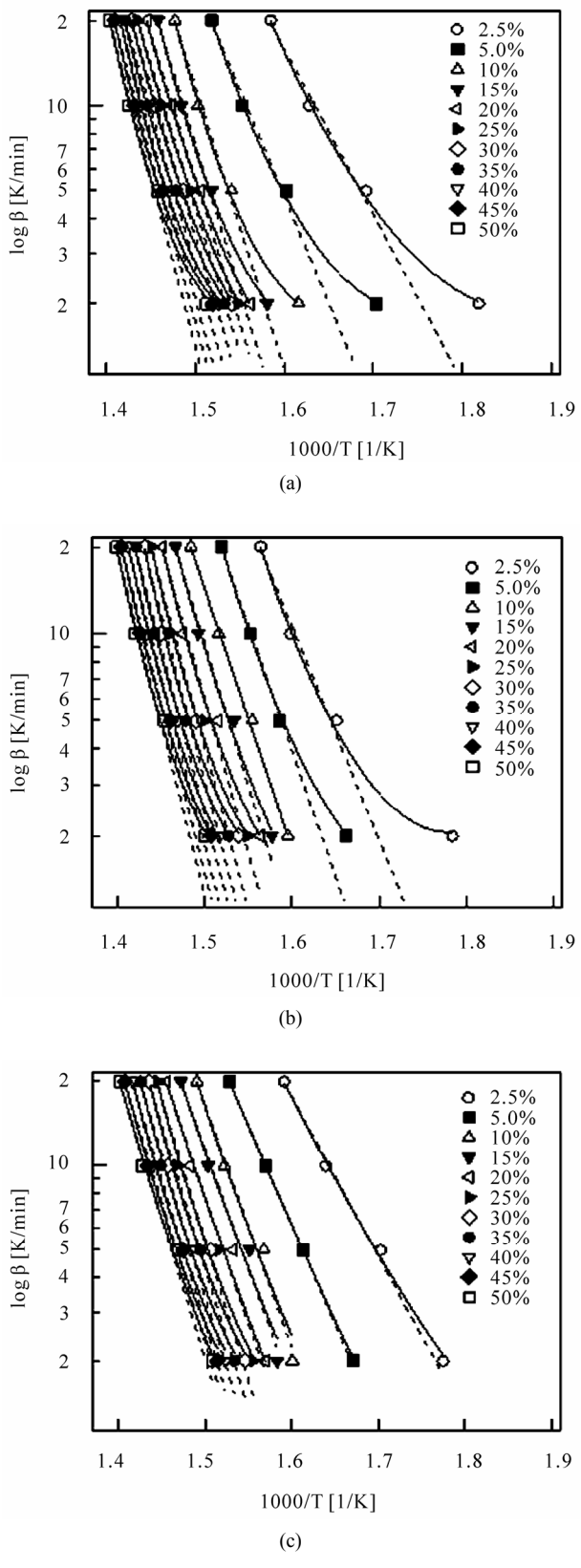

Figure 8. Flynn-Wall-Ozawa plot of (a) Unfilled (b) SOFTON filled and (c) CS filled RPET/RPP blends in air.

thermal oxidative decomposition.

The E_a of kinetic parameter for thermal oxidative degradation of these blends can be evaluated by using polynomial and linear coefficient from polynomial fitting data as shown in **Figure 9**. The E_a values at initial stage of thermal oxidative decomposition (E_a 0.05) are 124, 157 and 141 kJ/mol while E_a values at 50% weight loss (E_a 0.50) are 200, 214 and 162 kJ/mol as presented in **Table 3** for unfilled, SOFTON filled and CS filled REPT/RPP blends, respectively. The E_a values as a function of weight loss in **Figure 9** exhibited a two-step degradation profile of thermal oxidative degradation in air. The E_a values increased from the initial stage at 2.5 to 10% weight loss, which can be described as the first step of degradation. The E_a values gradually came to a plateau with further weight loss.

Thermal stability of the blends was improved with the incorporation of CS and SOFTON, which prompted an increment in E_a values, especially at the initial stages of degradation. This could be attributed to interaction between filler and polymer matrix and filler would act as barrier to protect volatile substance during decomposi-

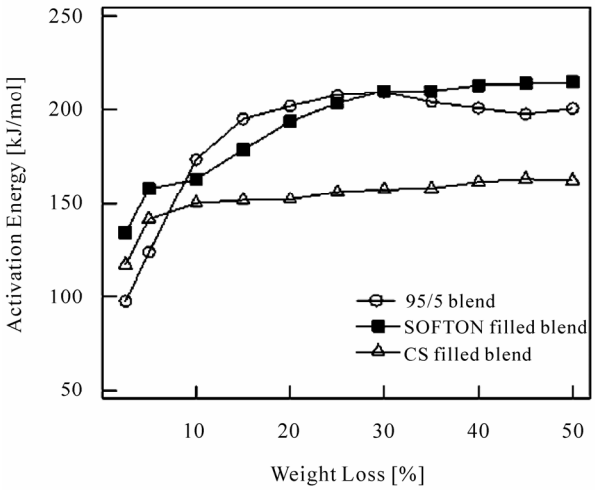

Figure 9. Activation energy of unfilled and filled RPET/RPP blends in air.

Table 3. Kinetic parameters of unfilled and filled RPET/RPP blends from the Flynn-Wall-Ozawa method.

Blend	Filler	Nitrogen		Air	
		$E_{a\,0.05}$	$E_{a\,0.50}$	$E_{a\,0.05}$	$E_{a\,0.50}$
		(kJ/mol)	(kJ/mol)	(kJ/mol)	(kJ/mol)
	-	225.1	237.5	124.2	200.3
95/5	SOFTON	218.6	220.4	157.8	214.8
	CS	191.7	227.8	141.6	162.3

Copyright © 2011 SciRes.

tion of these blends. The degradation of the blends would also depend on the state of dispersion of the RPP phase as well as the filler in the RPET matrix. Due to the low thermal stability of RPP in the presence of oxygen, the degradation of the blends would be slower when RPP is well dispersed and embedded within in the RPET matrix since the latter could become a good oxygen barrier. Moreover, well dispersed filler particles could also retard or inhibit thermal oxidative degradation by acting as a barrier to prevent attacks by volatile substances on the polymeric phases. However, thermal stability of the CS filled blends was slightly inferior to the unfilled and SOFTON filled blends, which could be due to the large CS particle size that prevented the formation of an effective barrier.

3.6. Thermal Decomposition Kinetic from Kissinger Model

Thermal decomposition kinetics based on the Kissinger method is calculated through the derivation from heterogeneous chemical reactions and widely used without considering the reaction order (n) or conversion function, f(α) [19]. The kinetic equation of the Kissinger model is expressed as

$$\ln\left(\frac{\beta}{T_{dm}{}^2}\right)=\ln\left(\frac{AR}{E_a f(\alpha)}\right)-\frac{E_a}{RT_{dm}} \quad (6)$$

where $f(\alpha)=n(1-\alpha_m)^{n-1}$, α_m is maximum conversion of weight, n is reaction order and T_{dm} is the highest degradation temperature of the first derivative of material at constant heating rate. The activation energy can be investigated by using the slope of ln (β/T^2_{dm}) versus $1/T_{dm}$ of Kissinger plot by

$$E_a=R\left[\frac{d\left(\ln\beta/T_{dm}^2\right)}{d\left(1/T_{dm}\right)}\right] \quad (7)$$

The pre-exponential factor can be obtained from the intercepts of the Kissinger plot.

The E_a values and pre-exponential factor (*ln* A) from Kissinger model as well as the degradation rate (dα/dt) are shown in **Table 4**.

From the results, E_a and *ln* A of the blends was lower when decomposed in air than in N_2, which was due to thermal oxidative degradation in the presence of oxygen. The highest thermal stability, as determined from the Kissinger model, was observed in SOFTON filled RPET/RPP blend, which exhibited high activation energy and pre-exponential factor. Similar to the results obtained through FWO, the CS filled composites also exhibited lower thermal stability than SOFTON filled composites as can be deduced from the lower E_a and *ln* A values determined by the Kissinger method. Nevertheless, both CS and SOFTON filled blends exhibited lower rate of degradation (dα/dt) as compared to the unfilled blends.

According to thermal decomposition kinetic study, kinetic parameter including activation energy, pre-exponential factor and reaction order of the blends can be influenced by various factors such as the kinetic methods, the sample mass and size, and the operating conditions [12]. Therefore, the kinetic compensation effect was developed in order to determine the effect from the different specimens or experimental conditions in a change of activation energy calculation [9]. In this circumstance, kinetic parameter of pre-exponential factor, A would vary with the activation energy, E_a. Form kinetic parameters of Kissinger models, linear plots between *ln* A and E_a of the unfilled and filled RPET/RPP blends is illustrated in **Figure 10** The compensation effect of these blends are based on thermal degradation under N_2 and air as determined by Equations (8) and (9), respectively

$$\ln A=-11.37+0.17E_a \quad (8)$$

$$\ln A=-8.85+0.16E_a \quad (9)$$

These linear relationships from thermal degradation and thermal oxidative degradation suggest that an isokinetic relationship between pre-exponential and activation energy was established whereby the thermal decomposition mechanisms of unfilled and filled RPET/RPP blends were similar [9]. It is interesting to note that decomposition atmosphere plays an important role on thermal decomposition kinetic of unfilled and filled

Table 4. Kinetic parameters of unfilled and filled RPET/RPP blends from the Kissinger method.

Blend	Filler	Nitrogen			Air		
		E_a (kJ/mol)	*ln* A (min^{-1})	*da/dt* (%/min)	E_a (kJ/mol)	*ln* A (min^{-1})	*da/dt* (%/min)
	-	225.1	27.53	10.43	159.0	16.54	9.27
95/5	SOFTON	206.4	24.26	9.03	175.9	19.20	6.72
	CS	203.4	23.60	9.08	159.3	15.53	6.52

Copyright © 2011 SciRes.

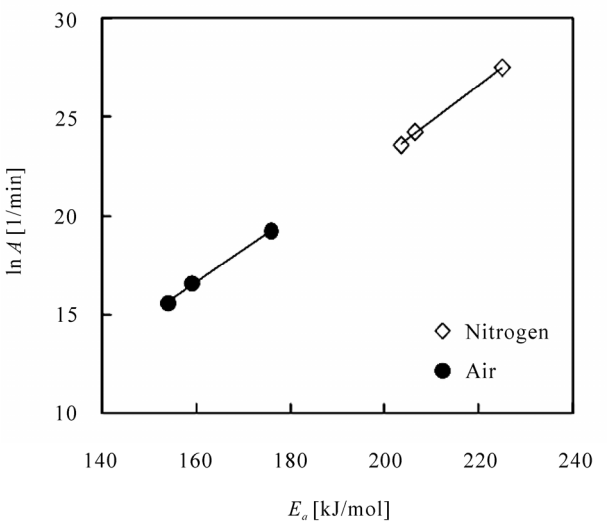

Figure 10. Linear relationship of *ln* A and E_a of unfilled and filled RPET/RPP blends in N_2 and air.

RPET/RPP blends, whereby the kinetic parameters during decomposition in N_2 were significantly higher than those recorded during thermal oxidative decomposition in the presence of oxygen.

3.7. Flame Retardant Property

Flame retardant property of CS and SOFTON filled blends was investigated by using the limiting oxygen index (LOI). The LOI values decreased with increasing filler concentration indicating higher flammability, as shown in **Table 5**. It was observed in the unfilled specimen that the region under the flame would melt instantaneously to cause dripping, which prevented the flame from spreading towards other parts of the specimen. The incorporation of $CaCO_3$, however, prevented this dripping thus causing the specimens to continue burning. It should be noted that flame retardants are generally added into polymers at high contents of up to 60 wt%. Therefore, it is thought that the amount of $CaCO_3$ incorporated into the blends may be insufficient to dilute the combustible portion of the blends. The thermal oxidative decomposition kinetic of the filled blends can also be useful to explain their flame resistance. The second step of thermal oxidative decomposition in the filled blends when exposed to air can be related to the deterioration of carbonaceous elements or char formed from the initial decomposition of organic substances. The presence of $CaCO_3$ would accelerate the decomposition of aromatic groups in the blend during degradation leading to faster formation of char, which would provide better flame resistance to the RPET/RPP blend. However, at low content of filler could not yield efficiency flame retardancy of the filled blends.

3.8. Mechanical Properties of $CaCO_3$ Filled RPET/RPP Blend

Table 5 summarizes the mechanical properties of unfilled and $CaCO_3$ filled RPET/RPP blends. The incorporation of fillers, both CS and SOFTON enhanced the stiffness and impact performance of the blend. The increment of tensile modulus (E) of the filled blend was due to the high rigidity of the filler particles whereas cavitation caused by the poor interfacial adhesion between fillers and the matrix could enhance their impact performances. Incidentally, the reduction in yield strength (σ) of the filled blends would also be due to the lack of interfacial adhesion between fillers and the blend matrix. It could be noted that CS filled blend exhibited highest modulus values due to the presence of aragonite crystal structures.

4. Conclusions

Thermal oxidative decomposition kinetics based on the FWO model was developed by using the second order polynomial equation, which fitted well with experimental data. The activation energy during thermal oxidative degradation was dependent on the size of fillers and RPP dispersed particles in the blends. According to the FWO model, a two-step degradation mechanism was observed when the samples were degraded in air. The incorporation of SOFTON provided higher thermal resistance to the blends especially at the first phase of degradation involving the deterioration of organic compounds. CS, however, did not act as an efficient thermal oxidative degradation barrier due to the large particle sizes. Meanwhile, the Kissinger kinetic model was able to suggest similar decomposition mechanisms in these blends through the linearity of the compensation plots. The incorporation of CS and SOFTON improved the thermal stability of RPET/RPP blends. However, char formation of both fillers was not enough for yield flame retardancy of the RPET/RPP blends. It is interesting to note that aragonite $CaCO_3$ of CS significantly enhance stiffness of the blends.

Table 5. Mechanical properties of unfilled and filled RPET/RPP blends limiting oxygen index (LOI).

Blend	Filler	E (GPa)	σ (MPa)	Impact strength (kJ/m^2)	LOI (%)
	-	1.54	46.5	1.54	23.5
95/5	SOFTON	1.78	43.0	1.77	20.3
	CS	1.99	42.6	1.09	20.4

Copyright © 2011 SciRes.

5. Acknowledgements

The authors gratefully acknowledge Dr. Hiroyuki Inoya, Yasuda Sanyo Co., Ltd., Japan for supporting materials and compounding system, Department of Industrial Engineering,Pathumwan Institute of Technology, Thailand for preparing cockleshell and Dr. Koji Yamada and Dr. Joji Kodata from Osaka Municipal Research Institute, Japan for limiting oxygen index measurement.

REFERENCES

[1] M. Heino, J. Kirjava, P. Hietaoja and J. Seppälä, "Compatibilization of Polyethylene Terephthalate/Polypropylene Blends with Styrene-Ethylene/Butylene-Styrene (SEBS) Block Copolymers," *Journal of Applied Polymer Science*, Vol. 65, No. 2, 1997, pp. 241-249. doi:10.1002/(SICI)1097-4628(19970711)65:2<241::AID-APP4>3.0.CO;2-O

[2] Y. X. Pang, D. M. Jia, H. J. Hu, D. J. Hourston and M. Song, "Effects of a Compatibilizing Agent on the Morphology, Interface and Mechanical Behaviour of Polypropylene/Poly (Ethylene Terephthalate) Blends," *Polymer*, Vol. 41, No. 1, 2000, pp. 357-365. doi:10.1016/S0032-3861(99)00123-8

[3] C. P. Papadopoulou and N. K. Kalfoglou, "Comparison of Compatibilizer Effectiveness for PET/PP Blends: Their Mechanical, Thermal and Morphology Characterization," *Polymer*, Vol. 41, No. 7, 2000, pp. 2543-2555. doi:10.1016/S0032-3861(99)00442-5

[4] N. H. de Leeuw and S. C. Parker, "Surface Structure and Morphology of Calcium Carbonate Polymorphs Calcite, Aragonite, and Vaterite: An Atomistic Approach," *The Journal of Physical Chemistry B*, Vol. 102, No. 16, 1998, pp. 2914-2922. doi:10.1021/jp973210f

[5] R. Gachter and H. Muller, "Plastics Additives Handbook," Hanser Publishers, Munich, 1990.

[6] K. M. Wilbur, "Physiology of Mollusca: Volume 1," Academic Press, New York, 1964.

[7] S. Keiko, Y. Tomohiko and T. Masami, "Synthesis of Aragonite from Calcined Scallop Shells at Ambient Temperatures and Their Morphological Characterization by FE-SEM," *Shigen-to-Sozai*, Vol. 118, No. 8, 2002, pp. 553-558. doi:10.2473/shigentosozai.118.553

[8] P. Budrugeac, "Application of Model-Free and Multivariate Non-Linear Regression Methods for Evaluation of the Thermo-Oxidative Endurance of a Recent Manufactured Parchment," *Journal of Thermal Analysis and Calorimetry*, Vol. 97, No. 2, 2009, pp. 443-451. doi:10.1007/s10973-009-0081-9

[9] D. S. Dias, M. S. Crespi, C. A. Ribeiro, J. L. S. Fernandes and H. M. G. Cerqueira, "Application of Non-Isothermal Cure Kinetics on the Interaction of Poly (Ethylene Terephthalate)—Alkyd Resin Paints," *Journal of Thermal Analysis and Calorimetry*, Vol. 91, No. 2, 2008, pp. 409-412. doi:10.1007/s10973-006-7862-1

[10] B. G. Girija, R. R. N. Sailaja and G. Madras, "Thermal Degradation and Mechanical Properties of PET Blends," *Polymer Degradation and Stability*, Vol. 90, No. 1, 2005, pp. 147-153. doi:10.1016/j.polymdegradstab.2005.03.003

[11] A. Khawam and D. Flanagan, "Solid-State Kinetic Models: Basics and Mathematical Fundamentals," *The Journal of Physical Chemistry B*, Vol. 110, No. 35, 2006, pp. 17315-17328. doi:10.1021/jp062746a

[12] J.-Y. Kim, D.-K. Kim and S.-H. Kim, "Thermal Decomposition Behavior of Poly (Ethylene 2,6 Naphthalate)/ Silica Nanocomposites," *Polymer Composites*, Vol. 30, No. 12, 2009, pp. 1779-1787. doi:10.1002/pc.20749

[13] S. Kim and J.-K. Park, "Characterization of Thermal Reaction by Peak Temperature and Height of DTG Curves," *Thermochimica Acta*, Vol. 264, No. 1-2, 1995, pp. 137-156. doi:10.1016/0040-6031(95)02316-T

[14] P. Paik and K. K. Kar, "Kinetics of Thermal Degradation and Estimation of Lifetime for Polypropylene Particles: Effects of Particle Size," *Polymer Degradation and Stability*, Vol. 93, No. 1, 2008, pp. 24-35. doi:10.1016/j.polymdegradstab.2007.11.001

[15] W. Tang, X. G. Li and D. Y. Yan, "Thermal Decomposition Kinetics of Thermotropic Copolyesters Made from *trans*-*p*-Hydroxycinnamic Acid and *p*-Hydroxybenzoic Acid," *Journal of Applied Polymer Science*, Vol. 91, No. 1, 2004, pp. 445-454. doi:10.1002/app.13103

[16] S. Ch. Turmanova, S. D. Genieva, A. S. Dimitrova and L. T. Vlaev, "Non-Isothermal Degradation Kinetics of Filled with Rise Husk Ash Polypropene Composites," *Express Polymer Letters*, Vol. 2, No. 2, 2008, pp. 133-146. doi:10.3144/expresspolymlett.2008.18

[17] S. Vyazovkin and C. Wight, "Isothermal and Nonisothermal Reaction Kinetics in Solids: In Search of Ways toward Consensus," *The Journal of Physical Chemistry A*, Vol. 101, No. 44, 1997, pp. 8279-8284. doi:10.1021/jp971889h

[18] L. Katsikas and I. G. Popović, "Improvement to the Flynn-Wall Method of Determining Apparent Activation Energies of the Thermal Degradation of Polymers," *The Journal of Physical Chemistry B*, Vol. 107, 2003, pp. 7522-7525. doi:10.1021/jp027865e

[19] J. A. F. F. Rocco, J. E. S. Lima, A. G. Frutuoso, K. Iha, M. Ionashiro, J. R. Matos and M. E. V. Suárez-Iha, "Thermal Degradation of a Composite Solid Propellant Examined by DSC," *Journal of Thermal Analysis and Calorimetry*, Vol. 75, No. 2, 2004, pp. 551-557. doi:10.1023/B:JTAN.0000027145.14854.f0

Copyright © 2011 SciRes.